

1 **Temperature dependence of non-thermal plasma assisted hydrocracking of toluene to**
2 **lower hydrocarbons in a dielectric barrier discharge reactor**

3 Faisal Saleem, Kui Zhang, Adam Harvey*

4 School of Engineering, Newcastle University Newcastle upon Tyne NE1 7RU

5 **Keywords:** gasification, tar, non-thermal plasma, dielectric barrier discharge

6 **Abstract**

7 Non-thermal plasma (NTP) is an attractive method for decomposing biomass gasification tars.
8 In this study, the removal of toluene (as a gasification tar analogue) was investigated in a
9 dielectric barrier discharge (DBD) reactor at ambient and elevated temperatures with hydrogen
10 as the carrier gas. This study demonstrated that higher temperature in the presence of a DBD
11 opens up new (thermal) reaction pathways to increase the selectivity to lower hydrocarbons via
12 DBD promoted ring-opening reactions of toluene in H₂ carrier gas. The effect of plasma power
13 (5 – 40 W), concentration (20-82 g/Nm³), temperature (ambient-400 °C) and residence time
14 (1.43-4.23 s) were studied. The maximum removal of toluene was observed at 40 W and 4.23
15 s. The major products were lower hydrocarbons (C₁-C₆) and solids. The synergetic effect of
16 power and temperature was investigated to decrease the unwanted solid deposition. It was
17 observed that the selectivity to lower hydrocarbons (LHCs) increased from 20 to 99.97 %, as
18 temperature was increased from ambient to 400 °C, at 40 W and 4.23 s. Methane, C₂ (C₂H₆ +
19 C₂H₄), and benzene were the major gaseous products, with a maximum selectivity of 97.93%
20 (60 % methane, 9.93 % C₂ (C₂H₆ + C₂H₄), and 28% benzene). It is important to note that
21 toluene conversion is not a function of temperature, but the selectivity to lower hydrocarbons
22 increases significantly at elevated temperatures under plasma conditions.

23

24 **1. Introduction**

25 Biomass can be used as an alternative source of “green” energy and chemicals. Biomass can
26 be converted into fuels and value-added chemicals by thermal, physical or biological processes.
27 Thermochemical processes are useful for producing fuels, chemicals, combined power and
28 heat. Among thermochemical processes, gasification is a promising technique for producing
29 alternatives, green fuels for transport and power generation. In this method, partial oxidation
30 of solid biomass is performed at temperatures of 700 to 800 °C, to produce gaseous fuels or
31 synthesis gas [1, 2]. The product gas contains high concentrations of CO and H₂. Its
32 composition depends upon various parameters such as the nature of the feedstock, method of
33 gasification, operating conditions, etc [2]. The syngas (CO + H₂) can be used as fuel in gas
34 turbines, gas engines, and it can be used to produce valuable chemicals. However, the product
35 gas from gasifier also has impurities such as chlorine, sulphur, nitrogen and tar compounds [3].
36 Among these, tar creates a significant problem by condensing in filter, heat exchangers and
37 engines at low temperatures after the exit of biomass gasifier, leading to attrition and choking.
38 Therefore, it is necessary to decompose or remove the tar compounds from the product gas [4].
39 There are numerous techniques that can be implemented to remove tars, such as mechanical
40 separation, thermal cracking, and catalytic cracking. Tar components can be reduced using
41 mechanical separation techniques such as Venturi scrubbers, rotational particle separators,
42 water scrubbers, ESP, and cyclones. However, these techniques only capture or remove the tar
43 compounds from gasifier product gas, thereby producing secondary pollution. In addition, the
44 associated chemical energy of the tar is wasted [5]. Thermal and catalytic techniques may be
45 used to crack tar compounds, but these methods have some drawbacks. In thermal cracking,
46 for instance, operating cost is significantly increased by maintaining the high temperature [6].
47 When using catalytic cracking, tar compounds can be cracked into valuable gaseous
48 compounds at lower temperatures than in thermal decomposition [7]. However, many catalysts

49 have high affinities for chlorine and sulphur, which can poison them. The main contaminants
50 in typical gasifier product gas are sulphur, chlorine and nitrogen compounds [8]. Therefore, it
51 is difficult to remove tar compounds completely, due to their complexity and variability and
52 unavailability of efficient and proven method.

53 Non thermal plasma (NTP) is widely considered to be an attractive solution for the
54 decomposition of volatile organic compounds (VOCs) and the production of fuels and
55 chemicals [9]. Downstream NTP treatment of tar has received considerable attention due to its
56 easy operation and compact design [10]. In NTP systems, the reactive species are derived from
57 the carrier gas via the impact of high energy electrons (1-10eV) [11]. This produces a variety
58 of reactive species (electrons, radicals and excited species), which can interact with the tar to
59 decompose the tar compounds. Various techniques have been employed to decompose the
60 biomass tar, often using toluene as a tar analogue. Combined plasma and catalysis techniques
61 can also be used to crack gasification tars. The plasma can reduce the catalyst's activation
62 energy and thereby increases the rate of decomposition of reactants, raising the yield and
63 possibly the selectivity of valuable gaseous products [12, 13]. Tao et al (2013) investigated the
64 plasma-assisted catalytic decomposition of a tar model compound (toluene) in a He carrier gas
65 using DC non-thermal pulsed plasma [14]. They reported that using plasma before the catalytic
66 steam reforming reactions enhanced the decomposition of toluene. It was observed that the
67 decomposition of toluene rises from 32 % to 57 % when using NTP before the catalyst bed
68 [14].

69 In another study, the presence of moisture increased the toluene decomposition efficiency in
70 air in a gliding arc discharge reactor [15]. In previous studies, it has been observed that removal
71 and energy efficacy of tar compound increases by adding the steam [16-19]. The decomposition
72 efficiency of toluene increased due to oxidation of toluene through OH radicals, which can

73 provide new reaction routes for the direct and indirect removal of toluene [17]. However,
74 addition of steam increases the operational cost and process complexity.

75 In this study, a DBD reactor was used to remove toluene in H₂ carrier gas. In our previous work
76 we reported almost complete conversion of tar (toluene) in CO₂ carrier gas, but with significant
77 formation of problematic solid residue occurred [20]. Toluene decomposition in H₂ has not
78 been reported in the literature, even though the product gas from gasification contains
79 significant amounts of H₂ (25.2-49.5 %) [21]. Therefore, for a better understanding of tar
80 removal from product gas, it is necessary to study the effect of H₂ on toluene conversion and
81 product selectivity in the NTP.

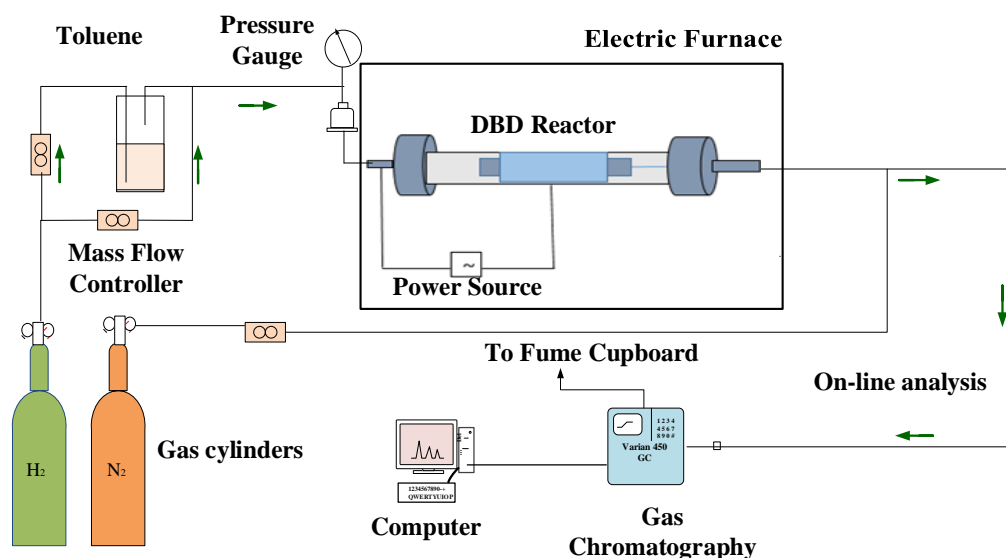
82 Toluene is one of the main stable compounds produced during biomass gasification process at
83 higher temperatures [22], and has been used in various experimental studies as a tar analogue
84 to investigate the removal efficiency [17, 18, 23-25]

85 The performance of the DBD reactor was also studied by varying power, toluene concentration,
86 temperature, and residence time. The present study reveals that the operation temperature plays
87 an important role in toluene conversion to lower hydrocarbons in H₂ carrier gas under NTP
88 conditions.

89 **2. Material s and methods**

90 **2.1 Experimental setup**

91 Fig.1 shows a schematic of the experimental setup. The coaxial dielectric barrier discharge



92

93

Fig.1. Schematic diagram of the experimental setup

94 (DBD) reactor consisted of two coaxial quartz tubes one inside the other. The two metal
 95 electrodes, one outside the external cylindrical quartz tube (330 mm length, 18 mm outer
 96 diameter, 15 mm inner diameter) and the other inside the inner tube (outer diameter 12 mm,
 97 inner diameter 10 mm). The inner and the outer metal mesh electrodes were made from 316
 98 stainless steel. The length of the external mesh was 45 mm resulting in a discharge region of
 99 about 2.86 cm³. The plasma was produced in the annular space between the coaxial cylindrical
 100 tubes. A variac was used to control the input voltage of the plasma generator which delivers
 101 power to DBD reactor. The voltage (0-20 kV peak-peak) and current signals were measured
 102 using an oscilloscope (TPS 2014B, Tektronix) to calculate the power transferred to the reactor.
 103 In this study, the power supplied to the DBD reactor was varied from 5 to 40 W, at a frequency
 104 of about 20 kHz.

105 Computer-controlled mass flow controllers regulated the flow rate of H₂ and N₂ from gas
 106 cylinders (BOC, UK, 99.99%), respectively. H₂ gas was saturated with toluene by passing
 107 through a bubbler (see Fig.1). The bubbler was placed in an ice bath to minimize the effect of
 108 diurnal fluctuations in ambient temperature on the rate of evaporation of toluene. The gas flow

109 rate was varied from 40.6 ml/min to 120 ml/min. To monitor the change of flow rate as a
110 consequence of plasma chemical reactions, a constant flow of nitrogen (6.0 mL/min) as
111 reference gas was added to the exit of the reactor. All values are stated at STP. To study the
112 effect of temperature on the performance of plasma chemical reactions, the plasma reactor was
113 placed inside a furnace which can adjust the temperature between ambient and 400°C.

114 The product compositions were monitored by a Varian 450-GC equipped with a TCD (Thermal
115 conductivity detector) to measure CH₄ and H₂, and a FID (Flame ionization detector) to
116 measure lighter hydrocarbons (LHC) including C₂ (C₂H₄, C₂H₆), C₃ (C₃H₆, C₃H₈), C₄ (C₄H₈,
117 C₄H₁₀), C₅ (C₅H₁₀, C₅H₁₂), and C₆H₆).

118 2.2 Definitions

119 The removal efficiency of toluene was defined as follows:

120

$$121 \quad d_T = \frac{\text{toluene in the input stream (mole/min)} - \text{toluene in the outlet stream (mole/min)}}{\text{toluene in input stream (mole/min)}} \times 100$$

122

123 The following formulae were used to calculate the selectivity of different LHC products:

124

$$125 \quad \text{LHC selectivity (\%)} = \frac{\sum (m \times \text{moles of } C_m H_n)}{7 \times \text{Moles of } C_7 H_8 \text{ converted}} \times 100$$

126 Where n and m are the carbon and hydrogen number respectively in the molecules

127 The SIE (specific input energy) shows the energy density applied to the plasma system

128

$$129 \quad \text{Specific input energy } \left(\frac{\text{kJ}}{\text{L}} \right) = \frac{P \text{ (W)} \times 60/1000}{\text{Flow rate total (L/min)}}$$

130

131 The energy efficiency was calculated as follows:

132

133
$$\text{Energy efficiency } \left(\frac{\text{g}}{\text{kWh}} \right) = \frac{\text{converted toluene (g/min)}}{P \text{ (W)} \times 60/3600000}$$

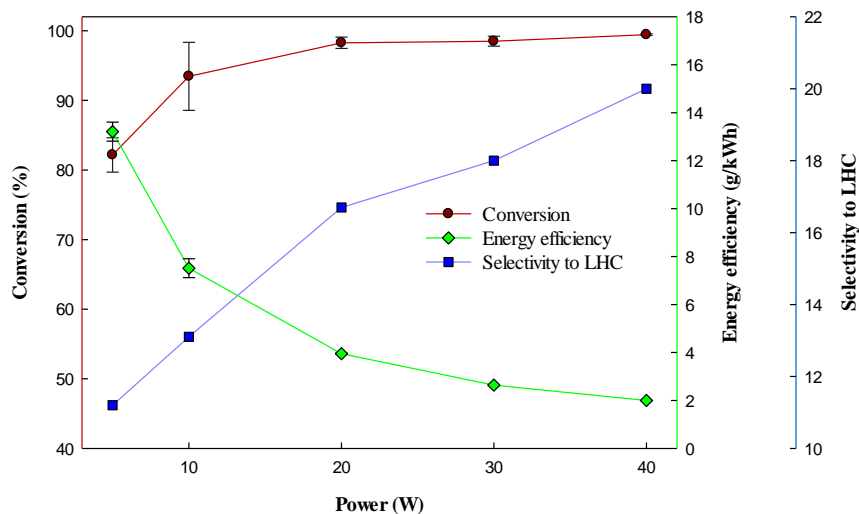
134

135 **3. Results and Discussion**

136 **3.1 Effect of Power**

137 The effect of power on the removal efficiency of toluene is shown in Fig.2 (a), below. Plasma
138 power was varied from 5 to 40 W (SIE =7.39-59.11 kJ/L). The initial concentration of toluene
139 was 33 g/m³, and the residence time was 4.23 s. It was found that toluene decomposition
140 efficiency increased with increasing plasma power, and the maximum removal of toluene was
141 99.5 % at 40 W and 4.23 s. The similar effect of power on the decomposition of toluene was
142 reported in previous experimental study [20, 26].

143 The energy efficiency and selectivity to LHCs are also shown in Fig.2 (a). The energy
144 efficiency of the plasma decomposition clearly decreases with increasing plasma power. There
145 are diminishing returns as the input power is increased. Similar trends have been reported for
146 the decomposition of tar analogue [16]. However, the overall selectivity of LHC increases from
147 11.20 to 20 % as the power was increased from 5 to 40 W, which suggested that the aromatic
148 ring was broken down at higher plasma power. Fig.2 (b) demonstrated that the selectivity of
149 LHCs (C₁-C₅) increased with increasing plasma power



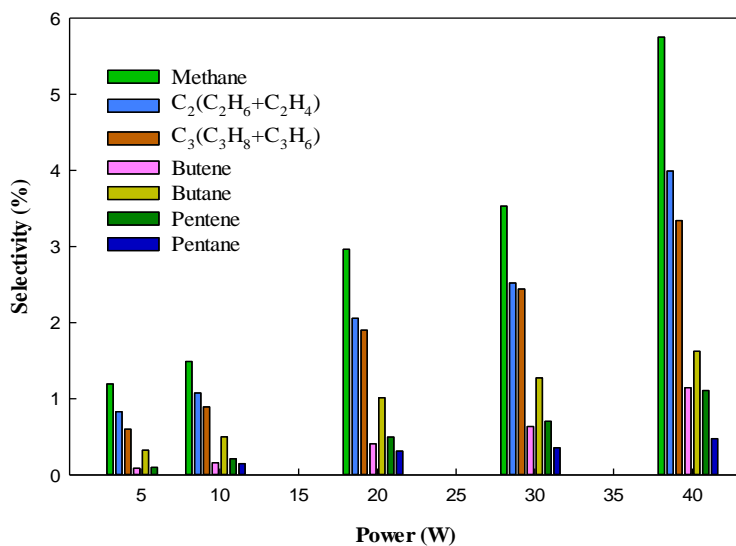
150

151 **Fig. 2(a)** Effect of plasma power on the conversion, energy efficiency and selectivity to LHC;

152 bars represent standard deviation. Reaction conditions: concentration = 33 g/Nm³;

153 Temperature=ambient; flow rate 40.6 ml/min; residence time= 4.23 s; and SIE=7.39-59.11

154 kJ/L.



155

156 **Fig.2 (b)** Selectivity of different LHC at 4.23 s. Reaction conditions: concentration = 33

157 g/Nm³; Temperature=ambient; residence time= 4.23 s; ; and SIE=7.39-59.11 kJ/L.

158 In a DBD plasma, the mean electron energy is in the range of 1-10 eV. The Maxwellian electron

159 energy distribution function (EEDF) shows the higher the average electron energy is, the more

160 electrons with higher energy will be produced [27]. These energetic electrons can generate
161 active radicals, ionic and excited atomic and molecular species through electron-impact
162 dissociation, ionization, and excitation of the source gases, i.e., H₂ and toluene, which can
163 initiate plasma assisted toluene decomposition/hydrocracking in H₂ carrier gas. The bond
164 dissociation energy of H₂ is 4.5 eV [28]. In a toluene molecule, the C-H bond dissociation
165 energy (3.7 eV) of the methyl group is lower than the dissociation energy of the C-H bond, and
166 C-C and C=C of the aromatic ring [28]. The bond dissociation energy of the C-C bond between
167 the aromatic ring and the methyl group is also higher (4.4 eV) [29, 30]. Therefore, initially, the
168 toluene could be decomposed via H-abstraction from methyl group, as well as aromatic ring
169 by electron impact dissociation of C-H bond in the molecule to form benzyl radical, because
170 the C-H bond in the methyl group and aromatic ring has lower dissociation energy. Moreover,
171 the energetic electrons could break the C-C bond between benzene ring and methyl group,
172 generating phenyl and methyl radicals [17]. The benzyl and phenyl radicals could agglomerate
173 to form solid residue. Meanwhile, these radicals (phenyl, and methyl radicals) could combine
174 with H radicals or react with H₂ to produce methane and benzene, respectively. The
175 agglomeration of methyl radicals can form higher hydrocarbons (such as C₂, C₃, C₄, C₅
176 hydrocarbons) [31, 32]. Another route for the decomposition of toluene is the cleavage of the
177 aromatic ring, which can produce LHCs (<C₆) directly by plasma assisted hydrocracking of
178 aromatic ring in an NTP[33]. “Therefore, both H radicals and energetic electrons contribute to
179 the decomposition of toluene in H₂ carrier gas. In an NTP, the formation of these chemically
180 reactive species is necessary for the tar decomposition/hydrocracking reactions. In the cracking
181 of a toluene molecule, the removal of methyl group, and the decomposition of aromatic ring
182 are important [33]. An increase in plasma power/voltage can increase the electric field strength
183 and the electron energy, which increases the number of reactive species in a DBD plasma. The
184 increased electric field strength, the electron density, and the higher energetic electrons at high

185 power/voltage could all contribute to the enhanced toluene conversion and the increased
186 selectivity of LHCs in an NTP.

187 It was observed that the NTP reactions strongly depended upon input energy. Hence, the
188 specific input energy (SIE) is the main factor affecting the performance of the plasma process.

189 It is reported that, even at 725 °C, the toluene conversion remains below 20 %, although the
190 complete decomposition occurs by 900 °C [25]. It was observed that the most favourable
191 required temperatures for toluene conversion was above 650 °C [22].

192 The decomposition of toluene with respect to SIE can be written as

193

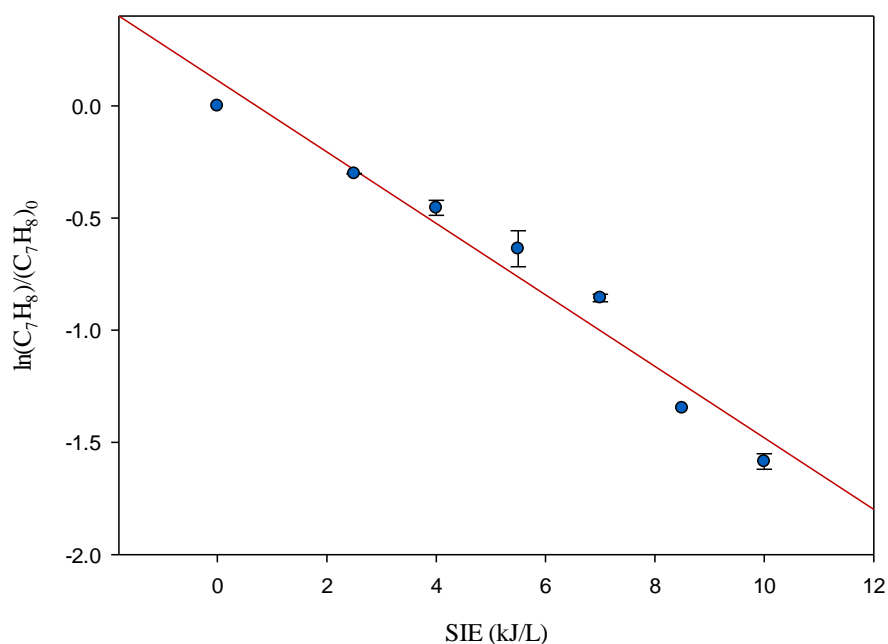
$$r = - d[C_7H_8]/ dSIE = k_{SIE}[C_7H_8]^n \quad (1)$$

194 Here n shows the reaction order and k_{SIE} is the energy constant in the given reaction. The natural
195 log of remaining fraction of the toluene with respect to SIE in H₂ carrier gas is shown in fig. 3.

196 It can be observed that the cracking of toluene in H₂ carrier gas can be represented by the
197 following equation.

198

$$\ln \frac{[C_7H_8]}{[C_7H_8]_0} = -k_{SIE} \times SIE$$



199

200

Fig.3 Effect of specific input energy (SIE) on the remaining fraction of toluene

201

(Reaction conditions: concentration = 33 g/Nm³; Temperature=ambient; and

202

residence time=1.43 s)

203

204

The values of the R² here is 0.96. Therefore, the cracking of toluene in dielectric barrier

205

discharge reactor as a function of SIE exhibits first order behaviour and the value of the energy

206

constant (k_{SIE}) is 0.16 (L/kJ). It was reported that electron impact plays a key role in NTPs in

207

similar reactions [30, 34].

208

209

3.2 Effect of concentration

210

The toluene concentration was varied between 20 and 82 g/Nm³, to observe the effect on the

211

conversion of toluene. Fig. 4 shows that the removal of toluene decreased from 98.5 % to 78%

212

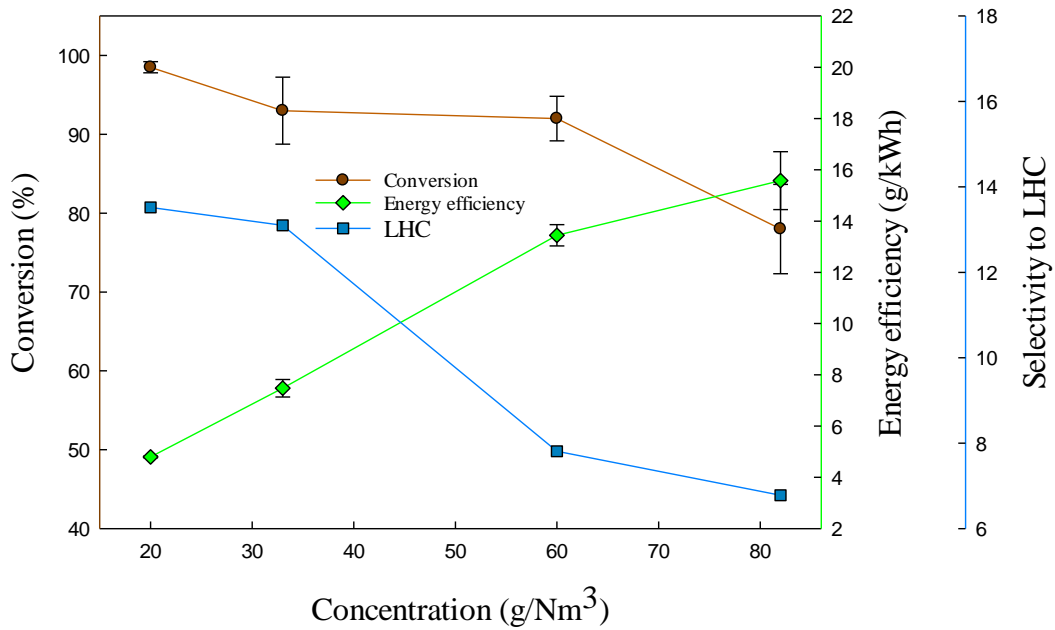
by increasing the concentration from 20 to 82 g/Nm³. The trend is consistent with previous

213

experimental results in which decomposition efficiency of toluene decreased with increasing

214

the concentration in a DBD plasma, and that for benzene in a gliding arc plasma [16, 20].



215

216 **Fig.4** Effect of concentration on the conversion of toluene and energy efficiency of the
 217 plasma process; bars represent standard deviation. Reaction conditions: input power=10 W;
 218 residence time=4.23 s; flow rate 40.6 ml/min; ambient temperature. ; and SIE=14.77 kJ/L

219 At constant power, the plasma-generated reactive species react with the toluene to decompose
 220 it. However, when the concentration is increased whilst keeping the others parameters constant,
 221 the relative amount of toluene molecules increases with respect to reactive species

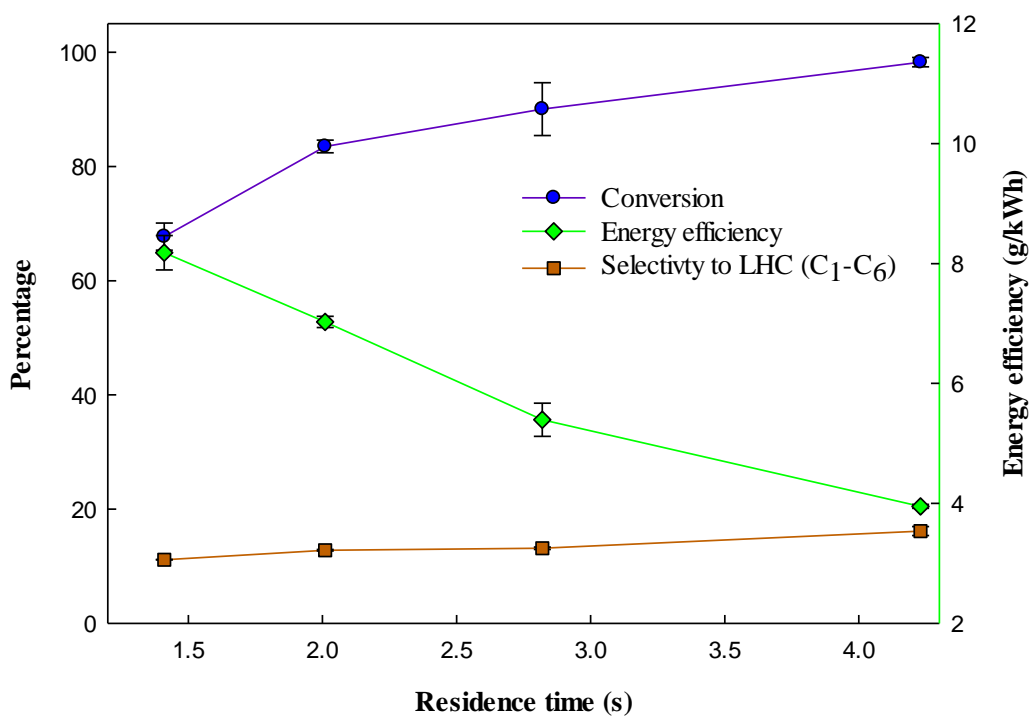
222 Therefore, as the concentration of toluene increases, the ratio of plasma-activated reactive
 223 species to toluene molecules will decrease, which will reduce the toluene conversion. Due to
 224 this reason, the selectivity to LHCs also decreases with increasing the concentration of toluene
 225 (Fig.4).

226 Fig.4 also shows the effect of the concentration of toluene on the energy efficiency of plasma.
 227 The energy efficiency increases from 4.79 g/kWh to 15.6 g/kWh by changing the concentration
 228 from 20 g/m³ to 82 g/Nm³. As the concentration is increased, it also increases the total amount
 229 of decomposed toluene, and so the energy efficiency of the plasma process.

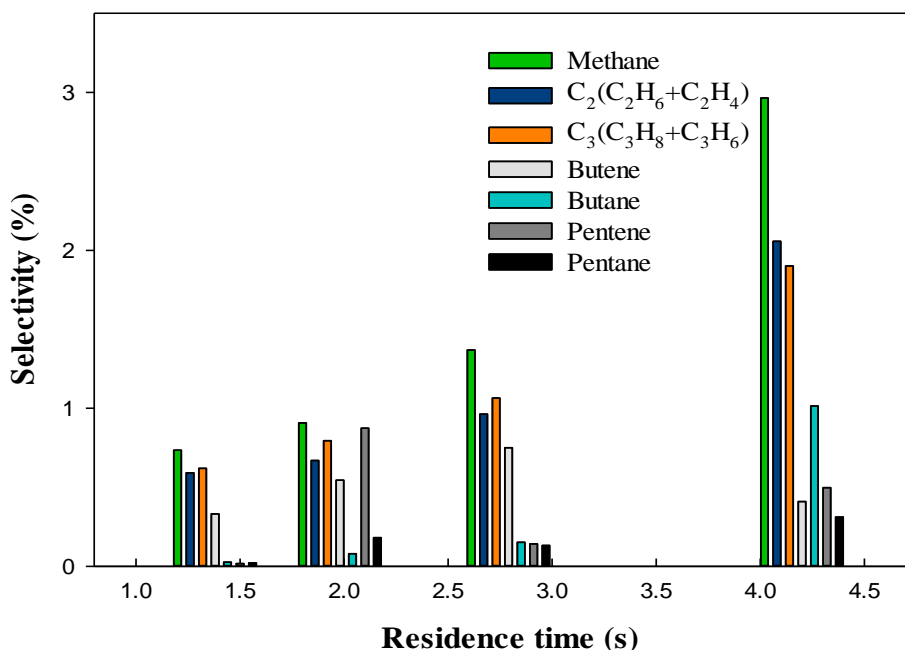
230 The trend is similar to previous work in which GAD (Gliding Arc Discharge) plasma [16] and
231 RGD (Rotating Gliding arc Discharge) plasmas [24] were used.

232 3.3 EFFECT OF RESIDENCE TIME

233 The removal efficiency of toluene is also influenced by residence time. Fig. 5 (a) shows the
234 effect of residence time on the conversion of toluene at 20 W. It can be observed that
235 decomposition of toluene increases with increasing residence time. The removal of toluene
236 continuously increases from 67 % to 98 % as the residence time increases from 1.43 s to 4.23
237 s at 20 W (SIE: 10-29.6 kJ/L). At high residence time, the tar compound and carrier gas are
238 subjected to plasma discharge zone for longer time, which can increase the collision between
239 reactive species and tar compound. Therefore, increasing residence time promotes the
240 conversion of toluene due to high number of collision between tar compounds and reactive
241 species [24]. The maximum conversion attained was 98 % at the highest residence time used
242 here (4.23 s).



243



245 **Fig.5** Effect of residence time (a) on the conversion of toluene, energy efficiency and
 246 selectivity to LHC; bars represent standard deviation (b) Selectivity to individual lower
 247 hydrocarbons. Reaction conditions: concentration = 33 g/Nm³; flow rate 40.6-120 ml/min;
 248 Temperature=ambient; and Power=20 W; and SEI=10-29.6 kJ/L

249 The energy efficiency and selectivity towards the lower hydrocarbons (C₁-C₆) are shown in
 250 Fig. 5 (a). The energy efficiency of the process decreases with increasing residence time. It can
 251 be seen that energy efficiency decreases from 7.9 g/kWh to 3.9 g/kWh with increasing
 252 residence time from 1.43 s to 4.23 s. A similar trend of decreasing flow rate has been reported
 253 on the conversion of benzene [16].The residence time is associated with the flow rate, and for
 254 high residence time flow rate needs to be reduced. At low flow rate, the amount of tar
 255 compound subjected to plasma reactor also decreases, which decreases the total amount of
 256 decomposed toluene. Therefore, at high residence time, energy efficiency of the system
 257 decreases due to reduction in the total amount of decomposed toluene. Fig.5 (b) shows that

258 selectivity of LHC ($C_1 - C_5$) increases with residence time. The H_2 carrier gas spends more time
259 in the plasma discharge with increasing residence time, which produces more H reactive
260 radicals. These H radicals may contribute to increases the selectivity of lower hydrocarbons by
261 reacting with toluene and its fragments.

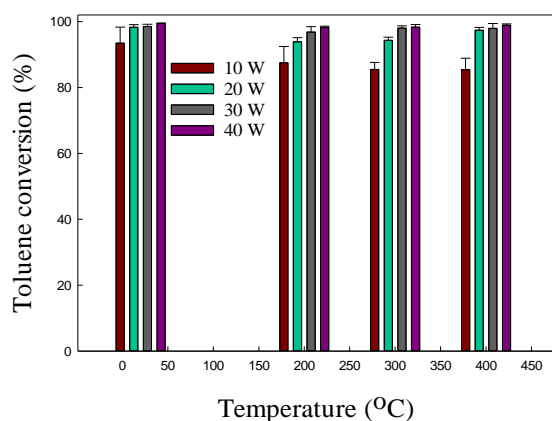
262 During the decomposition of toluene, a solid yellow residue was found inside the plasma zone.
263 In some reports, these deposits were described as polymeric substances, or carbonaceous
264 deposits [35, 36]. It was also reported that solid particles formed during the cracking of toluene
265 in air, leading to the formation of solid deposits on the surface of the catalyst, thereby
266 decreasing catalytic activity [37]. Moreover, formation of these solid residues can also clog the
267 reactor. Therefore, it is very important to avoid the deposition of solid residue. However, in
268 current study we have observed that the formation of solid residue completely disappeared (fig.
269 6 b) at elevated temperature in the presence of H_2 carrier gas.

270 **3.4 Effect of temperature**

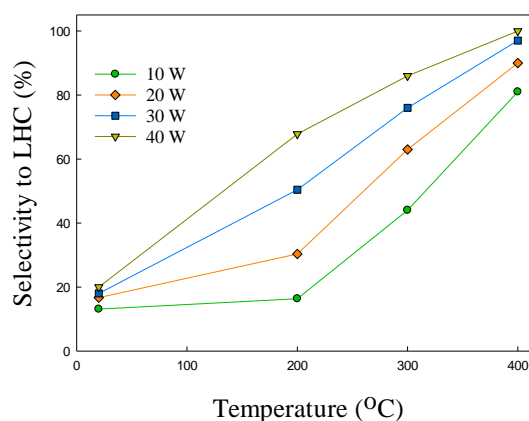
271 Experiments were conducted to investigate the effect of temperature on product distribution
272 and solid residue formation, at various powers (5-40 W) and a specific residence time (4.23 s).
273 Fig. 6 (a), below, shows that removal of toluene is not affected by increasing the temperature.
274 However, Song *et al.* (2002) reported that decomposition of toluene increased at elevated
275 temperatures [38]. In other research, it was demonstrated that elevated temperature increased
276 the removal efficiency of VOC in a non-thermal plasma reactor, and it was explained on the
277 basis of increased kinetic reaction rate of O radicals [39]. However, in those experiments air
278 was used as the carrier gas instead of H_2 . In this research, at 40 W, almost complete removal
279 of toluene was obtained at all temperatures.

280 Fig. 6 (b) shows the effect of temperature on the total selectivity to lower hydrocarbons at
281 various levels of power and 4.23 s, it can be seen that total selectivity significantly increases

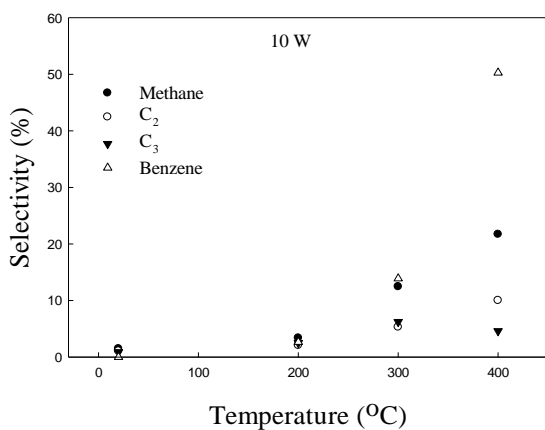
282 with increasing temperature at each level of power. At 400°C and 40 W, the selectivity rises
 283 from 20 % to 99.97 %, without the formation of solid residue. At 400°C and 4.23 s, the
 284 minimum selectivity towards LHC reaches to 81 % even at 10 W, which shows the high
 285 conversion of toluene to LHC, at high temperature, in the presence of H₂ carrier gas. There are
 286 three different types of reaction involve in hydrocracking of aromatics: (a) hydrogenation-
 287 dehydrogenation (b) isomerization and (c) cracking.



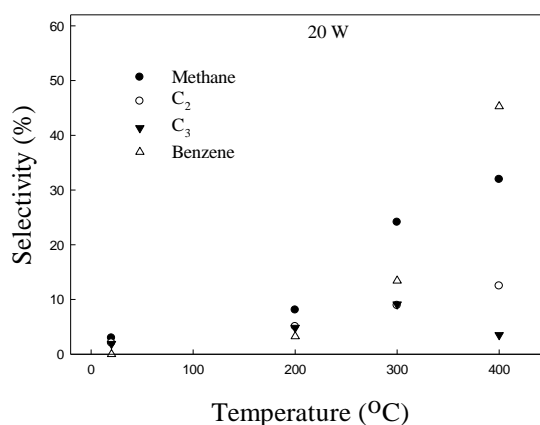
(a)



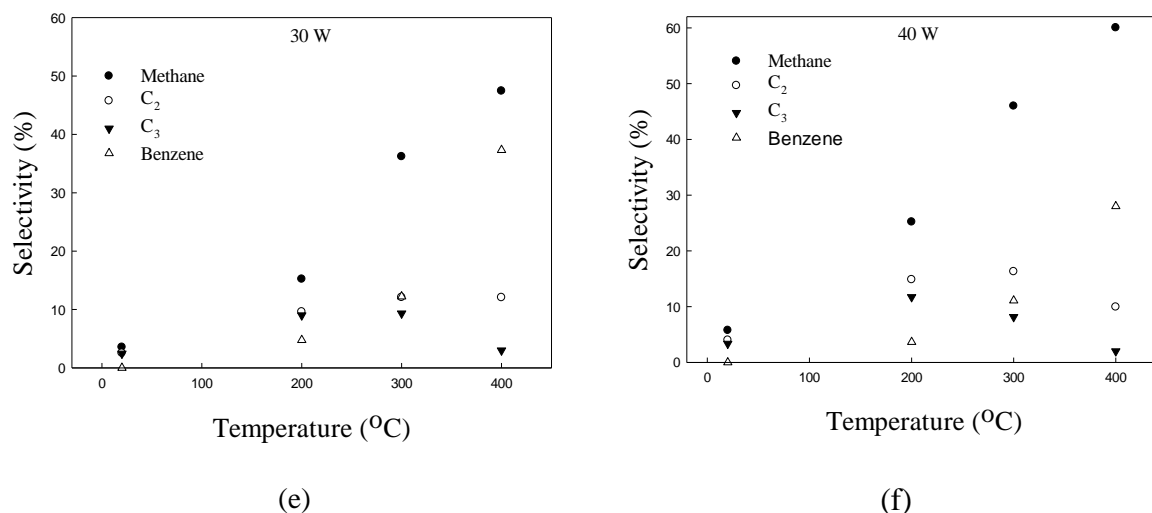
(b)



(c)



(d)



288 **Fig.6** Effect of temperature on: (a) the conversion of toluene; (b) Total selectivity LHC; (c)
 289 Selectivity to various LHCs at 10 W;(d) selectivity to various LHCs at 20 W;(e) selectivity to
 290 various LHCs at 30 W; and (f) selectivity to various LHCs at 40 W. Reaction conditions:
 291 concentration = 33 g/Nm³; flow rate 40.6 ml/min; residence time=4.23 s; and SIE=14.77-
 292 59.11 kJ/L

293 The cracking reaction can be categorized as primary (ring-opening), secondary and tertiary
 294 [40]. Hydrogenation and isomerization take place at lower temperature because of lower
 295 activation energy, whereas the rate of cracking (ring-opening) increases with increasing
 296 temperature [41].

297 Fig. 6(c), (d), (e), and (f) show the effect of temperature on the selectivity of individual LHCs
 298 at 10, 20, 30 and 40 W, respectively. Fig.6 (c) shows that, at 10 W, selectivity of benzene and
 299 methane reaches 50 % and 21% respectively, with increasing temperature up to 400 °C.
 300 However, the selectivity of C₂ (C₂H₆ + C₂H₄) and C₃ (C₃H₈+C₃H₆) remains below 11%. It has
 301 been reported that formation of benzene increases rapidly when increasing the temperature to
 302 400°C [42]. The high selectivity to the aromatic compounds may be due to a radical exchange
 303 reactions during the hydrocracking of toluene at high temperature [43]. It can be observed from
 304 fig. 6(f) that the selectivity of methane increases to 60%, whereas selectivity of benzene

305 reduces to 28%, at 40 W and 400°C. This happened due to the high population of energetic
306 electrons at high power. In the absence of plasma, the selectivity of methane was reported to
307 be nearly 10% at 450°C by hydrocracking of toluene [41]. It was reported that higher
308 temperatures (>850 °C) are required to produce CH₄ and C₂H₄ as the major gaseous products
309 [44, 45]. However, in this study, selectivity to methane reaches 60 % at 400 °C, due to the
310 additional effect of non-thermal plasma.

311 The selectivity of C₂ (C₂H₆ + C₂H₄) increases to 16.3 % by increasing the temperature up to
312 300°C, afterwards it decreases to 9.93 % at 400 °C. Similarly, the selectivity to C₃ (C₃H₈+C₃H₆)
313 increased when increasing the temperature from ambient to 200 °C, after which it decreased,
314 from 200 to 400 °C. This occurred because of formation of methane in the presence of excess
315 H₂ at high temperature [46]. Hence, the synergetic effect of plasma and temperature enhance
316 the selectivity to lower hydrocarbons rather than solid residue. Plasma causes the production
317 of reactive H radicals which hydrocrack toluene into lower hydrocarbons, when operating at
318 elevated temperatures. It has been reported that adding steam reduces the formation of solid
319 carbon and heavy hydrocarbons [47], which increase the operational cost and process
320 complexity. However in this study, it was noted that problem can instead be resolved using
321 hydrogen gas, which is already present (27-53 %) [48] in fuel product gas. The installation of
322 a DBD reactor at a suitable location after the gasifier exit, where the temperature was high
323 enough, could therefore have a substantial impact on tar mitigation.

324 **4. Conclusions**

325 In this study, the decomposition of toluene was studied in a dielectric barrier discharge (DBD)
326 reactor using H₂ as carrier gas, as a proxy for biomass gasification tars. For the first time, this
327 study investigated that elevated temperature in the presence of a DBD opens up new (thermal)
328 reaction pathways to raise the selectivity to lower hydrocarbons via DBD promoted ring-
329 opening reactions of toluene. H₂ was selected as a carrier gas because it is the major component

330 in most steam gasifier effluents. Experiments were performed at various levels of power (5-40
331 W) and residence time (1.43-4.23 s), at ambient and elevated temperature (20-400 °C), to
332 determine the conversion and selectivity towards valuable gaseous products.

333 The main findings are as follows:

- 334 i. The removal efficiency of toluene can be as high as 99.5 % in this design of DBD
335 reactor. The toluene is converted to lower hydrocarbons (C₁-C₆) and solid residue.
- 336 ii. The rate of decomposition of toluene increases with power input and residence time.
337 At ambient temperature, solid residue was formed in the reactor, which would create
338 various problems over time.
- 339 iii. Toluene conversion is not a function of temperature, but the selectivity is under plasma
340 conditions, which is different from conventional chemical process. The selectivity
341 towards lower hydrocarbons increases with increasing temperature, reaching 99.9 % at
342 400°C, without formation of solid deposits and heavy hydrocarbons (>C₆). Clearly,
343 there are benefits of combining thermal and non-thermal effects in this particular
344 application. Here, adding in thermal effects allows high selectivity to LHCs, without
345 solid residue formation: both desirable outcomes.
- 346 iv. Formation of methane, C₂ (C₂H₆ + C₂H₄) and benzene increases with increasing
347 temperature. Here, the maximum selectivities observed were 60%, 9.93 % and 28%,
348 respectively, at 400°C and 40 W (the highest values used).

349

350 **Acknowledgements**

351 The financial support is provided to first author by University of Engineering and Technology
352 Lahore, Pakistan to conduct PhD research, and from the Engineering and Physical Sciences

353 Research Council (EPSRC) Supergen Bioenergy Hub (EP/J017302/1) is gratefully
354 acknowledged.

355

356 **References**

357

- 358 [1] P. Basu, Biomass gasification and pyrolysis: practical design and theory, Academic press 2010.
359 [2] I. Narvaez, A. Orio, M.P. Aznar, J. Corella, Biomass gasification with air in an atmospheric bubbling
360 fluidized bed. Effect of six operational variables on the quality of the produced raw gas, Industrial &
361 Engineering Chemistry Research 35 (1996) 2110-2120.
362 [3] S. Anis, Z.A. Zainal, Tar reduction in biomass producer gas via mechanical, catalytic and thermal
363 methods: A review, Renewable and Sustainable Energy Reviews 15 (2011) 2355-2377.
364 [4] L. Devi, K.J. Ptasiński, F.J.J.G. Janssen, A review of the primary measures for tar elimination in
365 biomass gasification processes, Biomass and bioenergy 24 (2003) 125-140.
366 [5] Y. Richardson, J. Blin, A. Julbe, A short overview on purification and conditioning of syngas
367 produced by biomass gasification: catalytic strategies, process intensification and new concepts,
368 Progress in Energy and Combustion Science 38 (2012) 765-781.
369 [6] Y. Chen, Y.-h. Luo, W.-g. Wu, Y. Su, Experimental investigation on tar formation and destruction in
370 a lab-scale two-stage reactor, Energy & Fuels 23 (2009) 4659-4667.
371 [7] G.-Y. Chen, C. Liu, W.-C. Ma, B.-B. Yan, N. Ji, Catalytic Cracking of Tar from Biomass Gasification
372 over a HZSM-5-Supported Ni-MgO Catalyst, Energy & Fuels 29 (2015) 7969-7974.
373 [8] Y.N. Chun, M.S. Lim, Light tar decomposition of product pyrolysis gas from sewage sludge in a
374 gliding arc plasma reformer, Environmental Engineering Research 17 (2012) 89-94.
375 [9] X. Zhu, X. Gao, R. Qin, Y. Zeng, R. Qu, C. Zheng, X. Tu, Plasma-catalytic removal of formaldehyde
376 over Cu-Ce catalysts in a dielectric barrier discharge reactor, Applied Catalysis B: Environmental 170
377 (2015) 293-300.
378 [10] Q. Jin, B. Jiang, J. Han, S. Yao, Hexane decomposition without particle emission using a novel
379 dielectric barrier discharge reactor filled with porous dielectric balls, Chemical Engineering Journal
380 286 (2016) 300-310.
381 [11] K. Yan, E.J.M. Van Heesch, A.J.M. Pemen, P. Huijbrechts, F.M. Van Gompel, H. Van Leuken, Z.
382 Matyas, A high-voltage pulse generator for corona plasma generation, IEEE Transactions on Industry
383 Applications 38 (2002) 866-872.
384 [12] S.Y. Liu, D.H. Mei, Z. Shen, X. Tu, Nonoxidative conversion of methane in a dielectric barrier
385 discharge reactor: prediction of reaction performance based on neural network model, The Journal
386 of Physical Chemistry C 118 (2014) 10686-10693.
387 [13] X. Zhu, X. Gao, C. Zheng, Z. Wang, M. Ni, X. Tu, Plasma-catalytic removal of a low concentration
388 of acetone in humid conditions, RSC Advances 4 (2014) 37796-37805.
389 [14] K. Tao, N. Ohta, G. Liu, Y. Yoneyama, T. Wang, N. Tsubaki, Plasma enhanced catalytic reforming
390 of biomass tar model compound to syngas, Fuel 104 (2013) 53-57.
391 [15] C.M. Du, J.H. Yan, B. Cheron, Decomposition of toluene in a gliding arc discharge plasma reactor,
392 Plasma Sources Science and Technology 16 (2007) 791.
393 [16] Y.N. Chun, S.C. Kim, K. Yoshikawa, Decomposition of benzene as a surrogate tar in a gliding Arc
394 plasma, Environmental Progress & Sustainable Energy 32 (2013) 837-845.
395 [17] S. Liu, D. Mei, L. Wang, X. Tu, Steam reforming of toluene as biomass tar model compound in a
396 gliding arc discharge reactor, Chemical Engineering Journal 307 (2017) 793-802.

397 [18] S.Y. Liu, D.H. Mei, M.A. Nahil, S. Gadkari, S. Gu, P.T. Williams, X. Tu, Hybrid plasma-catalytic
398 steam reforming of toluene as a biomass tar model compound over Ni/Al₂O₃ catalysts, *Fuel*
399 *Processing Technology* 166 (2017) 269-275.

400 [19] Y.N. Chun, S.C. Kim, K. Yoshikawa, Removal characteristics of tar benzene using the externally
401 oscillated plasma reformer, *Chemical Engineering and Processing: Process Intensification* 57 (2012)
402 65-74.

403 [20] F. Saleem, K. Zhang, A. Harvey, Role of CO₂ in the Conversion of Toluene as a Tar Surrogate in a
404 Nonthermal Plasma Dielectric Barrier Discharge Reactor, *Energy & Fuels* (2018).

405 [21] S. Luo, B. Xiao, Z. Hu, S. Liu, X. Guo, M. He, Hydrogen-rich gas from catalytic steam gasification
406 of biomass in a fixed bed reactor: Influence of temperature and steam on gasification performance,
407 *International Journal of hydrogen energy* 34 (2009) 2191-2194.

408 [22] D. Swierczynski, C. Courson, A. Kiennemann, Study of steam reforming of toluene used as model
409 compound of tar produced by biomass gasification, *Chemical Engineering and Processing: Process*
410 *Intensification* 47 (2008) 508-513.

411 [23] J. Sun, Q. Wang, W. Wang, Z. Song, X. Zhao, Y. Mao, C. Ma, Novel treatment of a biomass tar
412 model compound via microwave-metal discharges, *Fuel* 207 (2017) 121-125.

413 [24] F. Zhu, X. Li, H. Zhang, A. Wu, J. Yan, M. Ni, H. Zhang, A. Buekens, Destruction of toluene by
414 rotating gliding arc discharge, *Fuel* 176 (2016) 78-85.

415 [25] G. Taralas, M.G. Kontominas, X. Kakatsios, Modeling the thermal destruction of toluene (C₇H₈)
416 as tar-related species for fuel gas cleanup, *Energy & Fuels* 17 (2003) 329-337.

417 [26] B. Wang, C. Chi, M. Xu, C. Wang, D. Meng, Plasma-catalytic removal of toluene over CeO₂-MnO
418 *x* catalysts in an atmosphere dielectric barrier discharge, *Chemical Engineering Journal* 322 (2017)
419 679-692.

420 [27] A. Michelmore, D.A. Steele, J.D. Whittle, J.W. Bradley, R.D. Short, Nanoscale deposition of
421 chemically functionalised films via plasma polymerisation, *Rsc Advances* 3 (2013) 13540-13557.

422 [28] B.d. Darwent, Bond dissociation energies in simple molecules, NSRDS-NBS NO. 31, U. S. DEPT.
423 COMMERCE, WASHINGTON, D. C. JAN. 1970, 48 P (1970).

424 [29] K. Urashima, J.-S. Chang, Removal of volatile organic compounds from air streams and industrial
425 flue gases by non-thermal plasma technology, *IEEE Transactions on Dielectrics and Electrical*
426 *Insulation* 7 (2000) 602-614.

427 [30] H. Kohno, A.A. Berezin, J.-S. Chang, M. Tamura, T. Yamamoto, A. Shibuya, S. Honda, Destruction
428 of volatile organic compounds used in a semiconductor industry by a capillary tube discharge
429 reactor, *IEEE Transactions on Industry Applications* 34 (1998) 953-966.

430 [31] K. Zhang, T. Mukhriza, X. Liu, P.P. Greco, E. Chiremba, A study on CO₂ and CH₄ conversion to
431 synthesis gas and higher hydrocarbons by the combination of catalysts and dielectric-barrier
432 discharges, *Appl. Catal., A* 502 (2015) 138-149.

433 [32] K. Zhang, B. Eliasson, U. Kogelschatz, Direct conversion of greenhouse gases to synthesis gas and
434 C-4 hydrocarbons over zeolite HY promoted by a dielectric-barrier discharge, *Industrial &*
435 *Engineering Chemistry Research* 41 (2002) 1462-1468.

436 [33] N. Blin-Simiand, F. Jorand, L. Magne, S. Pasquiers, C. Postel, J.R. Vacher, Plasma reactivity and
437 plasma-surface interactions during treatment of toluene by a dielectric barrier discharge, *Plasma*
438 *Chemistry and Plasma Processing* 28 (2008) 429-466.

439 [34] K. Urashima, J.S. Chang, T. Ito, Reduction of NO/_x from combustion flue gases by
440 superimposed barrier discharge plasma reactors, *IEEE Transactions on industry applications* 33
441 (1997) 879-886.

442 [35] M. Magureanu, D. Piroi, N.B. Mandache, V.I. Pârvulescu, V. Pârvulescu, B. Cojocaru, C. Cadigan,
443 R. Richards, H. Daly, C. Hardacre, In situ study of ozone and hybrid plasma Ag-Al catalysts for the
444 oxidation of toluene: evidence of the nature of the active sites, *Applied Catalysis B: Environmental*
445 104 (2011) 84-90.

446 [36] O. Karatum, M.A. Deshusses, A comparative study of dilute VOCs treatment in a non-thermal
447 plasma reactor, *Chemical Engineering Journal* 294 (2016) 308-315.

448 [37] V. Demidiouk, S.I. Moon, J.O. Chae, Toluene and butyl acetate removal from air by plasma-
449 catalytic system, *Catalysis Communications* 4 (2003) 51-56.

450 [38] Y.-H. Song, S.-J. Kim, K.-I. Choi, T. Yamamoto, Effects of adsorption and temperature on a
451 nonthermal plasma process for removing VOCs, *Journal of electrostatics* 55 (2002) 189-201.

452 [39] M.C. Hsiao, B.M. Penetrante, B.T. Merritt, G.E. Vogtlin, P.H. Wallman, Effect of gas temperature
453 on pulsed corona discharge processing of acetone, benzene and ethylene, *Journal of Advanced*
454 *Oxidation Technologies* 2 (1997) 306-311.

455 [40] M.A. Arribas, A. Martinez, The influence of zeolite acidity for the coupled hydrogenation and
456 ring opening of 1-methylnaphthalene on Pt/USY catalysts, *Applied Catalysis A: General* 230 (2002)
457 203-217.

458 [41] P. Castaño, J.M. Arandes, B. Pawelec, M. Olazar, J. Bilbao, Kinetic modeling for assessing the
459 product distribution in toluene hydrocracking on a Pt/HZSM-5 catalyst, *Industrial & Engineering*
460 *Chemistry Research* 47 (2008) 1043-1050.

461 [42] A. Amano, O. Horie, N.H. Hanh, Reaction of toluene with hydrogen atoms at elevated
462 temperatures, *Chemistry Letters* 1 (1972) 917-920.

463 [43] A. Amano, H. Tominaga, H. Tokuhisa, Mechanism of Thermal Hydrogenolysis of Toluene, *Bulletin*
464 *of The Japan Petroleum Institute* 7 (1965) 59-63.

465 [44] A. Jess, Mechanisms and kinetics of thermal reactions of aromatic hydrocarbons from pyrolysis
466 of solid fuels, *Fuel* 75 (1996) 1441-1448.

467 [45] C. Gai, Y. Dong, P. Fan, Z. Zhang, J. Liang, P. Xu, Kinetic study on thermal decomposition of
468 toluene in a micro fluidized bed reactor, *Energy Conversion and Management* 106 (2015) 721-727.

469 [46] J. Freel, A.K. Galwey, Hydrocarbon cracking reactions on nickel, *Journal of Catalysis* 10 (1968)
470 277-289.

471 [47] P. Jamróz, W. Kordylewski, M. Wnukowski, Microwave plasma application in decomposition and
472 steam reforming of model tar compounds, *Fuel Processing Technology* 169 (2018) 1-14.

473 [48] M. He, Z. Hu, B. Xiao, J. Li, X. Guo, S. Luo, F. Yang, Y. Feng, G. Yang, S. Liu, Hydrogen-rich gas
474 from catalytic steam gasification of municipal solid waste (MSW): influence of catalyst and
475 temperature on yield and product composition, *International Journal of Hydrogen Energy* 34 (2009)
476 195-203.

477